Quaternary Geochronology 71 (2022) 101319

Contents lists available at ScienceDirect

Quaternary Geochronology

journal homepage: www.elsevier.com/locate/quageo

Controls on luminescence signals in lake sediment cores: A study from Lake Suigetsu, Japan

Charlie L. Rex [a,*], Richard A. Staff [a], David C.W. Sanderson [a], Alan J. Cresswell [a], Michael H. Marshall [b], Masayuki Hyodo [c], Daishi Horiuchi [d], Ryuji Tada [d], Takeshi Nakagawa [e]

[a] Scottish Universities Environmental Research Centre (SUERC), University of Glasgow, Scottish Enterprise Technology Park, Rankine Avenue, East Kilbride, G75 0QF, UK
[b] Institute of Geography and Earth Sciences, Aberystwyth University, Aberystwyth, SY23 3DB, UK
[c] Research Center for Inland Seas, Kobe University, Kobe, 657-8501, Japan
[d] Department of Earth and Planetary Sciences, University of Tokyo, Hongo, Bunkyo-ku, Tokyo, 113-0033, Japan
[e] Ritsumeikan University, 1-chōme-1 Nojihigashi, Kusatsu, Shiga, 525-0058, Japan

ARTICLE INFO

Keywords:
Portable OSL
Laboratory profiling
Luminescence dating
Lake sediment
Palaeoenvironment

ABSTRACT

The luminescence characteristics of sediments are driven by a range of environmental factors and can be used as indicators of both local and regional environmental shifts. Hence, rapid luminescence profiling techniques are increasingly employed during multiproxy analysis of sediment cores, overcoming the practical limitations of traditional (dating) methods. One emerging application of luminescence profiling is in the palaeoenvironmental investigation of lake cores. This study demonstrates the versatility of rapid core profiling using portable optically stimulated luminescence and laboratory profiling techniques for appraising the luminescence characteristics of the Lake Suigetsu (Japan) sediment cores. These techniques were employed across four key time periods, each selected for their unique environmental context and significance on either a local or global scale, in order to identify relationships between down-core luminescence and environmental change. We demonstrate that the luminescence characteristics of the cores are susceptible to a range of environmental perturbations and can therefore act as proxies of past change. Additionally, the quantification of these luminescence signals, alongside an assessment of dose rate variations down-core, supports the notion that future luminescence dating is feasible. The results of this analysis contribute to the wider understanding of the application of luminescence techniques – both profiling and dating – to lake sediment cores.

1. Introduction

Optically Stimulated Luminescence (OSL) dating is a versatile chronological tool which can be applied to both marine and terrestrial sediment cores (e.g., Kadereit et al., 2012; Gao et al., 2017). The use of this technique has been aided by well-defined methodologies for extracting OSL-appropriate (light-tight) samples from core material (Armitage and Pinder, 2017; Nelson et al., 2019). OSL dating is often applied to complement other chronological tools, such as radiocarbon dating, during age-depth model construction (Zhao et al., 2019; Li et al., 2020). However, where other chronometers cannot be applied (e.g., if the material is older than the limit of radiocarbon dating), OSL dating can form a major component of the core chronology (e.g., Long, 2012; Hu et al., 2018).

However, the value of luminescence techniques to core analysis is not limited to dating alone (Munyikwa et al., 2021). It has been widely observed that the luminescence characteristics of sediments are driven by a range of environmental factors. Hence, down-core luminescence characterisation has the potential to contribute to our understanding of environmental change through time. However, most traditional luminescence techniques are both time- and core material-intensive (Bateman and Catt, 1996; Stone et al., 2015), which limits the number of samples that it is feasible to analyse and delays the final output of results until some months after sampling (Porat et al., 2019). As a result, rapid luminescence profiling techniques are increasingly employed to characterise the luminescence behaviour of core sediments and elucidate environmental changes, typically as part of multiproxy analysis (e.g., Ghilardi et al., 2015; Sanderson and Kinnaird, 2019; Pears et al., 2020).

* Corresponding author.
E-mail address: c.rex.1@research.gla.ac.uk (C.L. Rex).

https://doi.org/10.1016/j.quageo.2022.101319
Received 1 December 2021; Received in revised form 1 April 2022; Accepted 19 April 2022
Available online 29 April 2022

In this study, we examine the versatility of rapid down-core profiling techniques (portable OSL (POSL) analysis and laboratory (lab) profiling) for the detection of luminescence proxies of environmental change in lake sediment cores (from Lake Suigetsu, Japan). Such luminescence proxies have only recently been investigated in a lacustrine setting for this purpose (Píšková et al., 2019). Variations in luminescence characteristics (both natural signals and sensitivities) are examined and compared to known environmental shifts, supported by existing proxy data. The Suigetsu cores offer a unique opportunity to probe this relationship across a ~140,000-year age range in a lacustrine setting. A secondary aim of our study was to provide an assessment of the dating potential of the Suigetsu core material across a range of ages by comparing the quartz and polymineral fractions as potential chronometers, and to identify complexities which could hinder future age calculations. The motivation for this aspect of the work was the extension of the absolute Suigetsu chronology beyond the limit of radiocarbon dating.

The luminescence characteristics of the Suigetsu cores were appraised during four key time periods, each selected for their distinctive environmental context and significance on either a local or global scale. This facilitates the examination of a range of prominent environmental shifts on the luminescence characteristics of the cores, following the logic that the most pronounced shifts would cause changes that are most easily detectable by the chosen methods. The time periods span almost the full temporal range of the Suigetsu cores, including sections both covered by the existing radiocarbon chronology (in order to tether our findings in a chronologically well-constrained period) and older than the radiocarbon limit (to consider the potential of Suigetsu for future dating). The youngest of these (Time Period 1, "the Last 500 Years") spans from ~550 cal BP to the present day; a period comprising a series of local environmental perturbations, including the artificial connection of the lake to the Sea of Japan and a number of local flood events. The next (Time Period 2, "the Laschamp Excursion") extends from ~45,000 to 35,000 cal BP; a period of global change containing the Laschamp geomagnetic excursion and variable average annual temperatures (concomitant with Greenland Interstadials 12 to 7; Rasmussen et al., 2014). The third time period (Time Period 3, "the Varve Limit") spans from ~73,000 to 69,000 yr BP and is centred on the initiation of varving, which represents a significant alteration in lake biogeochemistry. The final time period (Time Period 4, "Termination II") extends from ~140,000 to 118,000 yr BP, encapsulating the global transition from MIS 6 to MIS 5e, which is associated with broadly increasing temperatures and a strengthening Summer Monsoon in East Asia (Duan et al., 2019).

2. Regional setting

Suigetsu is a tectonic lake located on the western side of the active Mikata fault in Fukui Prefecture, Honshu Island, central Japan (35° 35′ N, 135° 53′ E; Supplementary Fig. 1). The western side of the fault is subsiding and hence the lake has deepened through time. During late-MIS 7/early-MIS 6, Suigetsu was a transient shallow fluvial-lacustrine environment (Nakagawa et al., 2012), which became a brackish lake during the MIS 5e global sea level highstand. Diatom assemblage analysis indicates that the lake experienced freshwater conditions from MIS 5d to the Holocene. In the present day, the lake is ~34 m deep and brackish, having been artificially connected to the Sea of Japan via the Urami Canal (Supplementary Fig. 1) in 286 cal BP (AD 1664; Saito-Kato et al., 2013).

The Suigetsu sediments are continuously, countably varved between ~10,000 and ~50,000 cal BP, providing the longest such record from the Quaternary (Schlolaut et al., 2018). Varve counting, coupled with a radiocarbon dataset consisting of over 800 measurements (Staff et al., 2011; Bronk Ramsey et al., 2012) and tephra tie points (e.g., McLean et al., 2018; Albert et al., 2019) constitute the robust core chronology to 50,000 cal BP, which is aligned to the IntCal20 timescale (Bronk Ramsey et al., 2020). Beyond 50,000 cal BP, a provisional chronology is loosely constrained by wiggle matching of *Cryptomeria* pollen from Suigetsu to the LR04 benthic stack.

Four previous coring campaigns (SG93, SG06, SG12 and SG14) recovered a series of overlapping sediment core sections from the present day to >200,000 yr BP (98 m of composite depth; Nakagawa et al., 2012; McLean et al., 2018). The preserved sequence encapsulates two glacial and two full interglacial periods of continuous sedimentation. Any effects of disturbance are minimal; the presence of laminations during MIS 5e and varves between ~70,000 yr BP and the present day (indicating bottom water anoxia and good conditions for preservation) and further sedimentological inspection suggests that the core material does not contain hiatuses or disturbed sections (Nakagawa et al., 2012). This provides a palaeoenvironmental archive that comprises well-preserved millennial, centennial, decadal, annual, and even sub-annual-scale environmental oscillations which are the subject of ongoing multiproxy analysis. The Suigetsu cores are suitable for luminescence analysis because they contain detrital particles which have remained in-situ within the sequence post-deposition.

3. Materials and methods

3.1. Core materials

Materials were obtained from the SG06 cores for luminescence characterisation, totalling 60 samples. To mitigate against exposure of samples to light prior to measurement, the top 1 mm of sediment was removed from longitudinally split cores under dim red-light conditions to access unexposed material. Beyond this depth the influence of natural light has been shown to be smaller than the analytical error, so this material was deemed suitable for analysis (Armitage and Pinder, 2017). Sampling strategies varied based on availability of material, duration of time period, and structure of the event(s) to be studied (Supplementary Information 1). Contiguous (continuous adjacent) sampling was employed for Time Periods 1 and 3, because these spanned shorter intervals. Spot sampling was employed for Time Periods 2 and 4.

In addition, six samples were subsequently taken from across the four time periods for estimated dose rate (ED_R) determination. These samples were analysed to compare the selected mineral fractions as potential chronometers and identify ED_R variations down-core which could affect the POSL and lab profiling results. These were taken post-luminescence analysis; one sample from each time period at a depth associated with representative natural luminescence values, and two additional samples at positions in the stratigraphy associated with relatively elevated natural luminescence values (within Time Periods 2 and 3).

3.2. Sample analysis

Each sample was subjected to two sets of analysis. First, measurements of IR- and blue light-stimulated luminescence were conducted using a POSL system (Supplementary Information 2). Each sample was spread to cover a 5 cm diameter Petri dish (ensuring a consistent exposed surface area for all samples) and then subjected to a Continuous Wave Proxy (CWproxy) measurement scheme to yield a suite of analytical values (Sanderson and Murphy, 2010; Kinnaird et al., 2015). These values comprised: two net quantities (POSLnet and PIRSLnet; calculated from total photon counts under blue-light and IR stimulations respectively, a proxy for age, sensitivity and dose rate); two depletion indices (Depletion Index (Blue) and Depletion Index (IR); calculated from the difference between the total photon count during the first and second 30 s of blue/IR stimulation, a proxy for mineralogical change, bulk properties and previous bleaching extent); and a PIRSL/POSL ratio (calculated by taking a ratio of the POSLnet and PIRSLnet values, a proxy for mineralogical change; Supplementary Information 2). Empty chamber measurements were taken every two samples to check for contamination in the instrument. A measurement of the POSL standards

(Morar Sand and Granulite) was taken at the start and end of each ~12-sample batch to verify instrument performance.

Second, samples underwent lab profiling, which consisted of a short chemical preparation before measurement in a Risø TL/OSL system (TL-DA-15; Supplementary Information 3 and Supplementary Fig. 2; Burbidge et al., 2007; Sanderson and Murphy, 2010). Chemical pretreatment isolated two fractions: a Polymineral Fine (PMF) fraction, comprising mixed mineralogy grains ~5–50 μm in size; and a Quartz Fine (QF) fraction, comprising HF etched material (predominantly quartz; although some samples contained some larger feldspar grains), again 5–50 μm in size. Two aliquots were measured per fraction as a monolayer on an 11 mm diameter disc. The Risø outputs were used to determine an estimated equivalent dose (ED_e) in Gy by using the natural signal and the response of each aliquot to a 50 Gy dose (5 Gy doses were also included in the measurement scheme, but the relatively low sensitivity of the material precluded use of the response to such doses during sensitivity assessment). Each PMF aliquot was measured under both IR and blue light (yielding PMF-IR and PMF-blue signals, respectively), and the QF aliquots were measured under blue light only (to give a QF-blue signal).

The six samples for ED_R determination were dried and homogenised by grinding prior to measurement of key elemental concentrations following the procedure in Olive et al. (2001). A set of five standards were run alongside the samples (consisting of incremental ratios of Basalt:Granulite (1:0, 3:1, 1:1, 1:3, 0:1)). Elemental concentrations of uranium (U) and thorium (Th) were determined by Inductively Coupled Plasma Mass Spectrometry (ICP-MS) and potassium (K), iron (Fe) and manganese (Mn) by Inductively Coupled Plasma Optical Emission Spectrometry (ICP-OES). ED_R values were calculated using microdosimetry (Supplementary Information 4; Supplementary Table 2). The QF-blue, PMF-IR and PMF-blue ED_e values were considered alongside the ED_R values in order to resolve first-order age approximations that can be compared to the existing Suigetsu chronology.

4. Results and interpretation

4.1. Time Period 1, the last 500 years

Signals from both the POSL and lab profiling were small in magnitude for the last 500 years, reflecting the young age of the sediments (Fig. 1). Most samples contained only small quantities of quartz; hence data collection from the QF fraction was limited to a minority of discs and no clear trends were observed. The transition from fresh to brackish water in Suigetsu had no detectable influence on the luminescence properties of the sediment, and all variables remained constant across this boundary. Flood layers (visible as pale layers in the core photograph and highlighted in orange in Fig. 1) had the greatest impact on the luminescence profiles, producing high amplitude peaks at approximately −30 cal BP (AD 1980) and 120 cal BP (AD 1830) in the POSLnet and PIRSLnet profiles (Fig. 1A), which correspond with elevated ED_e values from lab profiling (Fig. 1C). This suggests that across this section, POSLnet, PIRSLnet and PMF ED_e can be used as an indicator of the presence of flood-related material. These peaks were not observed in either of the depletion indices, nor in the PIRSL/POSL ratio (Fig. 1B), suggesting that they cannot be attributed to mineralogical variations and are unlikely to have resulted from different bleaching histories, and instead that these samples contained residual elevated dose values. The preservation of these elevated signals could be a result of delivery of this material in a manner that did not expose it to light, such as slumping of water-saturated hillsides, or large volumes of suspended sediments in river flow.

One sample (highlighted in yellow in Fig. 1) that did not visually correlate with flood layers or produce large POSLnet or PIRSLnet values did nevertheless exhibit large ED_e values (predominately as a result of high natural signals), however the aliquots were inconsistent. This sample corresponded to a peak in titanium (Ti) content, as measured by

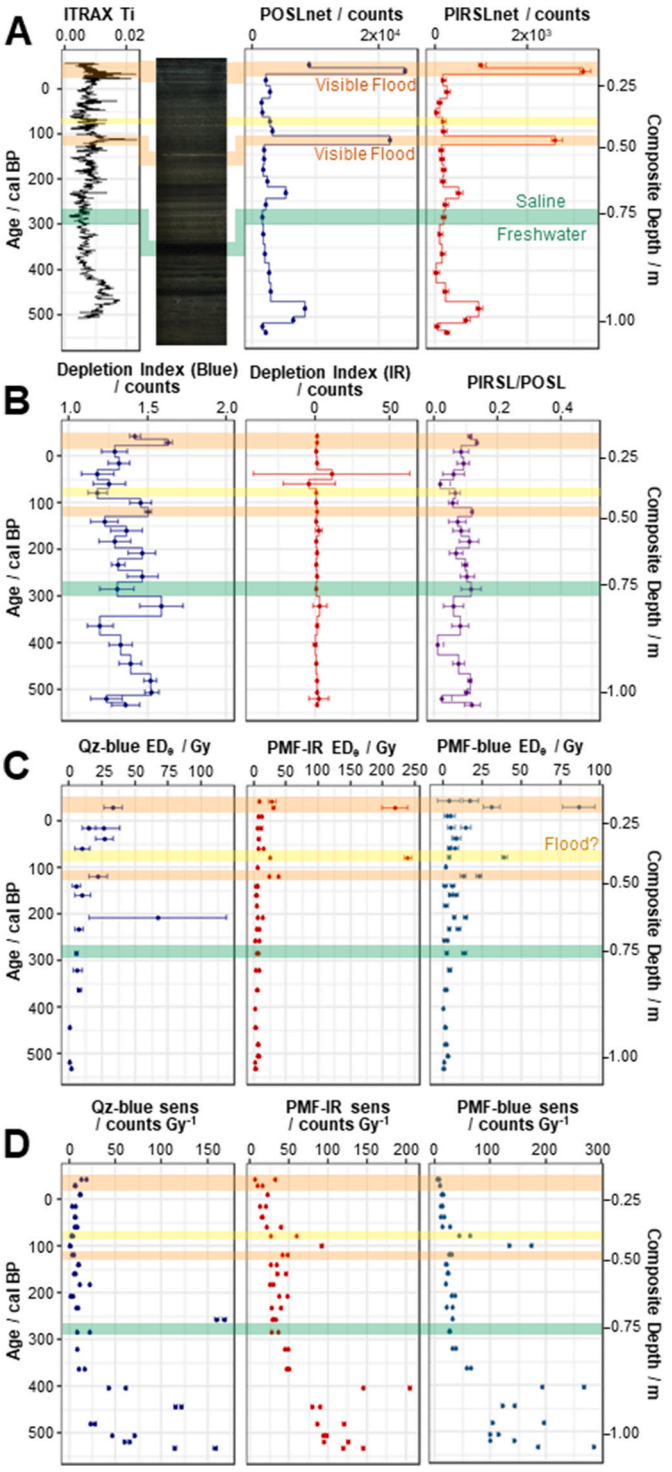

Fig. 1. Results of the POSL (Panels A and B) and lab profiling (Panels C and D) analysis for the 24 samples in Time Period 1. Panel A also shows contextual data (core photograph and ITRAX XRF Ti (Marshall et al., 2012)). Visible flood layers are highlighted in orange. An additional posited flood layer is highlighted in yellow. The transition from fresh to brackish lake water during 286 cal BP (AD 1664) is highlighted in green.

ITRAX X-ray fluorescence (XRF) analysis (Marshall et al., 2012; Fig. 1A). In Suigetsu, Ti can be interpreted as a proxy for detrital in wash, which suggests that this sample also contained flood material (despite there being no large visible flood layer) that resulted in elevated ED_e values. This disparity between lab profiling aliquots may be attributable to a relatively small volume of flood material within the sample, which was

not exposed during measurement in the POSL reader, and then unevenly partitioned between aliquots as grains were randomly loaded onto the discs for measurement, yielding different signal magnitudes during lab profiling.

A relatively high Ti content was also observed at the base of the profile, and whilst this did not correlate with elevated ED_e values, the samples taken from this period were associated with higher PMF sensitivities under both IR and blue light (Fig. 1D). This suggests that this older material had a distinct source-possibly the hillsides surrounding the lake as opposed to delivery via Lake Mikata (which acts to filter large detrital grains)- but that the delivery mechanism into the lake was more gradual than that of the flood material described above (encouraging bleaching prior to burial, and thus smaller ED_e values).

4.2. Time Period 2, the Laschamp Excursion

The POSLnet and PIRSLnet profiles across Time Period 2 showed two key transitions-one to a larger net signal at the Laschamp geomagnetic excursion itself (~42,000 cal BP) and a second to a smaller net signal at ~39,000 cal BP (Fig. 2A). Much like Time Period 1, there were no fluctuations in the depletion indices or the PIRSL/POSL ratio that corresponded to these transitions (Fig. 2B), suggesting that this trend was not driven by mineralogical variations or bleaching histories. Additionally, there was no clear relationship between these variables and the pollen-derived temperature reconstruction (Fig. 2A). This suggests that there was no obvious connection between temperature and core luminescence characteristics, despite the variability of the climate during this period.

The lab profiling-derived ED_e profiles (Fig. 2C) presented similar trends to the POSLnet and PIRSLnet with some subtle variations in the shape of the profile. In the ED_e profiles, the younger (~39,000 cal BP) shift was greater in magnitude than the older (~42,000 cal BP) shift, and in the QF-blue profile, only the younger shift was beyond the margin of error. Unlike the POSLnet and PIRSLnet, the PMF ED_e profiles were not smooth, with the excursion only consisting of two samples (at 39,500 cal BP and 40,500 cal BP). ED_R values calculated for this material suggest that it was associated with an elevated dose rate (~0.3–0.5 mGy/yr greater than the underlying material), but not sufficiently elevated to account for the ~100–200 Gy difference in the PMF ED_e values. Despite the sensitivities varying significantly between aliquots, the ED_e values were consistent within each aliquot pair. This suggests that these trends were not reflecting a signal from a very short event within each sample window, and instead a signal that is common to the bulk of each sample (as statistically, the likelihood of even loading of aliquots is lower for events which form a smaller proportion of the sample volume).

Whilst this positive excursion in ED_e values does not coincide directly with the magnetic field reversal during the Laschamp geomagnetic excursion, it aligns with a ~3000-year period of higher relative palaeointensity (normalised depositional remanent magnetism) (Fig. 2A, Hyodo et al., 2022). This apparent correlation is of note at the sampling resolution used in this study. Confirming this observation with higher resolution luminescence characterisation and supporting evidence for a mechanism linking these variables will be the focus of future work.

4.3. Time Period 3, the varve limit

A marked shift in a number of variables was observed across the varve limit (between 71,500 yr BP and 71,000 yr BP; Fig. 3), with samples taken from the varved sediment exhibiting larger POSLnet and PIRSLnet (Fig. 3A), ED_e values (Fig. 3C) and sensitivities (Fig. 3D) than the underlying non-varved sediment. The two samples taken from within the transitional clay produced intermediate signals between these end members. The transition from low to high ED_e was most dramatic in the PMF-IR and PMF-blue profiles despite the younger samples also showing higher sensitivities, however the QF-blue ED_e profile also showed elevated values post-transition. The different luminescence characteristics observed in each sedimentological regime suggest a significant shift in catchment conditions during this period, however there were no distinct changes in the depletion indices or

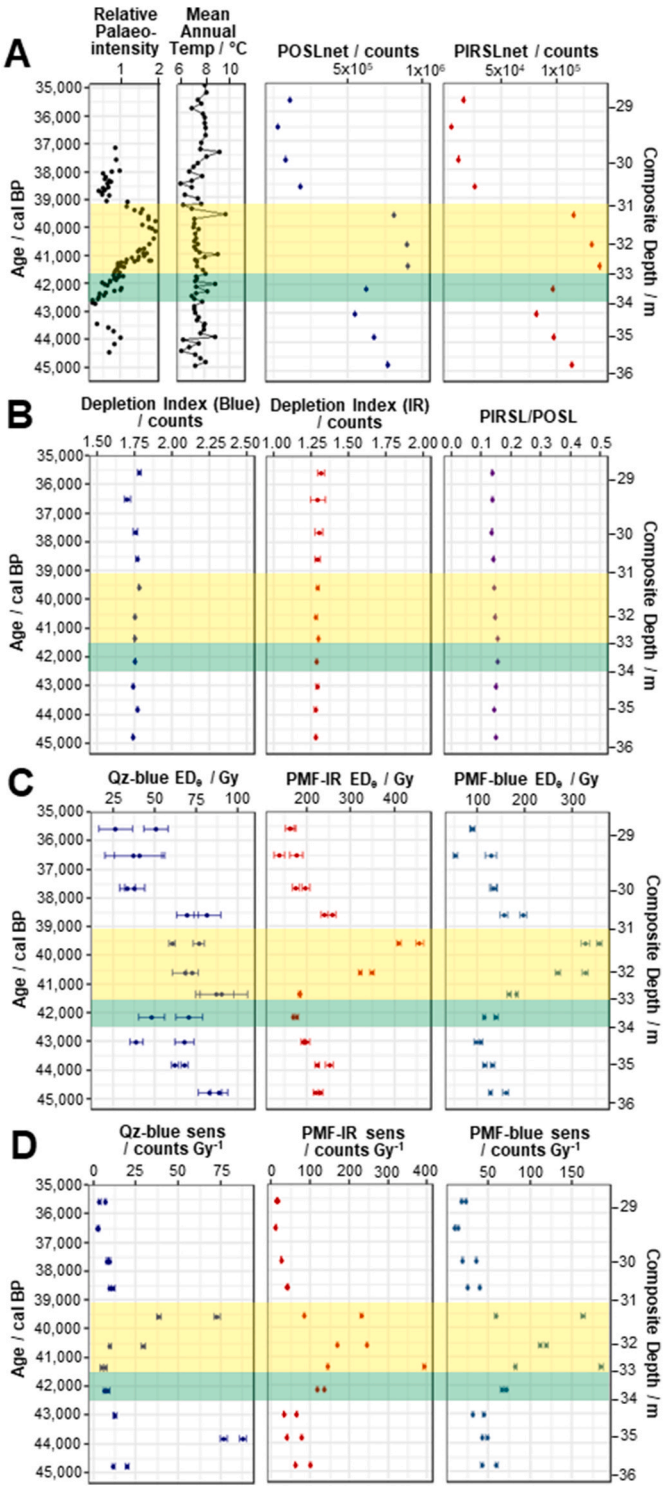

Fig. 2. Results of the POSL (Panels A and B) and lab profiling (Panels C and D) analysis for the 11 samples in Time Period 2. Panel A also shows contextual data (relative palaeointensity ($J_{200°C}/\chi_{200°C}$; Hyodo et al., 2022) and pollen-reconstructed mean annual temperature from Suigetsu). Green horizontal bars highlight the Laschamp geomagnetic excursion. Yellow horizontal bars highlight the period of higher relative palaeointensity following the Laschamp.

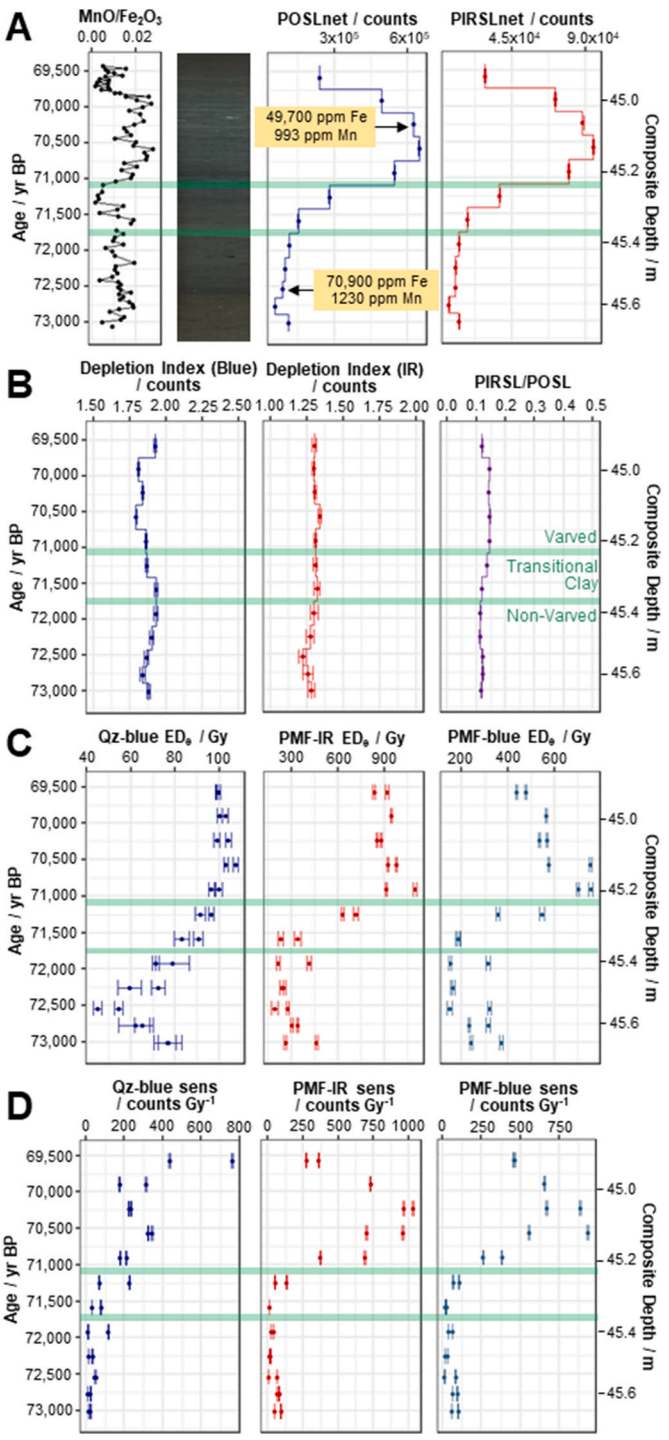

Fig. 3. Results of the POSL (Panels A and B) and lab profiling (Panels C and D) analysis for the 12 samples in Time Period 3. Panel A also shows contextual data (core photograph, MnO/Fe_2O_3, measured on a Horiba XGT-2700 and Fe and Mn contents from ICP-OES (yellow boxes)). Green horizontal bars bracket the transitional clay layer, which separates varved from non-varved sediment.

PIRSL/POSL ratio, suggesting that changes in mineralogy and dose history did not contribute to the variations in POSLnet, PIRSLnet and ED_e (Fig. 3B).

The conflicting presence of higher ED_e values in the younger sediment may be associated with a change in dose rate resulting from abrupt changes to lake chemistry. It is thought that varve formation was initiated in Suigetsu due to an abrupt deepening of the lake (possibly due to movement of the adjacent Mikata fault) which induced bottom water anoxia (Nakagawa et al., 2012), a process which is associated with incomplete mixing during lake overturning. This change in oxygenation (and therefore redox conditions) is corroborated by large differences in Fe and Mn concentrations above and below the onset of varving, as detected in the ICP-OES measurements, and an increase in the MnO/Fe_2O_3 ratio (Fig. 3A). The varved sediments also contain elevated U, Th and K concentrations in relation to the underlying non-varved sediment (Supplementary Table 1), resulting in a factor of ~2 increase in the ED_R which, when applied to the ED_e values in Fig. 3, aligns the first-order age approximations of the varved and non-varved sediment, supporting the thesis that the observed variation in ED_e is one driven by dose rate. It is possible that the change in redox conditions at this transition resulted in this enrichment of radiogenic elements, however, further assessment of decay series disequilibria and the time-dependency of chemical alterations (including U-enrichment) is required to better characterise this transition.

4.4. Time Period 4, Termination II

The POSLnet and PIRSLnet profiles for Termination II were broadly similar in shape, and both measures showed an overall increase with depth (Fig. 4A). There were some small anomalies in the blue depletion index and the PIRSL/POSL ratio (Fig. 4B) corresponding to some of the more extreme net values, which suggests that such values could be driven by different bleaching histories or mineralogical variations (changing quartz contents). It was not possible to determine sensitivity and ED_e values for all samples due to low mineral abundances and sensitivities. Where it was achievable, the values were shown to be highly variable between aliquots, between measurement techniques, and through time (Fig. 4C and D).

Termination II covers the broadest time range in this study and thus variability was anticipated, given the multiple high-amplitude environmental and sedimentological variations occurring during this transition from cold to warm temperatures. Suigetsu itself was non-static during this period, and sedimentological evidence suggests that it transitioned from fluvio-lacustrine in MIS 6 to lacustrine (and brackish) during MIS 5e, representing a dynamic environment both physically and geochemically. Another possible contributor to the lack of distinct trends is the implementation of spot sampling at low resolution over a large age range, which can result in additional noise (as samples capture extremes of environmental conditions without context from adjacent material). Despite it being difficult to isolate individual influences without relevant complementary data from sedimentological analysis, these observations suggest that the luminescence characteristics of this sediment are sensitive to a variety of competing environmental factors which could include lake depth, catchment drainage patterns, lake geochemistry, sediment source, flood events and climatic factors.

4.5. Estimated dose rates

The ED_R values showed down-core variations as a result of changing elemental concentrations, estimated water content and cosmic dose rate (Supplementary Table 1). The values were on the order of ~1–3 mGy/yr (Supplementary Table 2). When the ED_R values are considered alongside the ED_e values from the lab profiling, differences between chronometers are apparent; both the QF-blue and the PMF-blue ED_e values yield first order approximate ages which are broadly consistent (within an order of magnitude) with the existing Suigetsu ages across Time Periods 2–4, with the former underestimating age for ED_R values approaching the upper bound (~3 mGy/yr) and the latter typically overestimating age for the ED_R values approaching the lower bound (~1 mGy/yr). The ED_e values derived from the PMF-IR measurements consistently overestimate the existing Suigetsu ages, and the signals from all three fractions overestimate the true age of the sediment from Time Period 1. Constraining ages beyond these tentative observations would be erroneous, given the uncertainties in ED_R calculation (namely assumptions

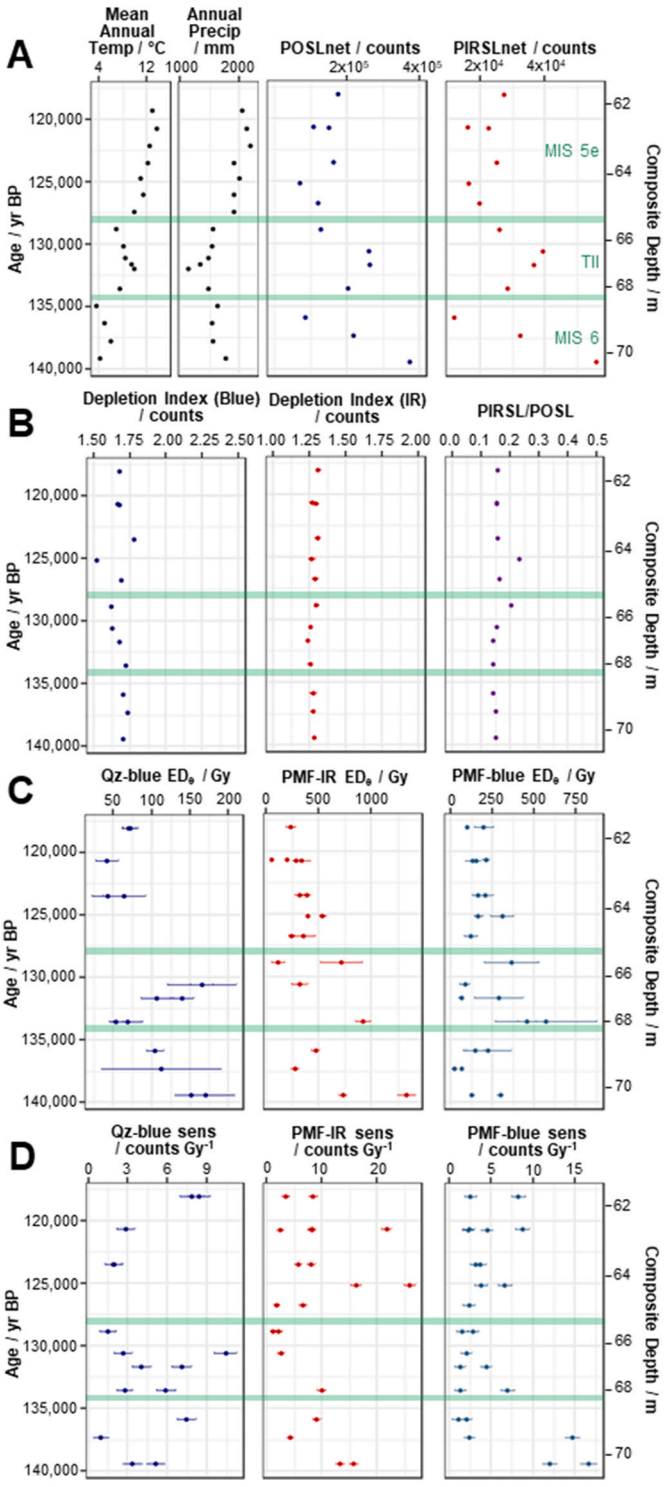

Fig. 4. Results of the POSL (Panels A and B) and lab profiling (Panels C and D) analysis for the 13 samples in Time Period 4. Panel A also shows contextual data (pollen-reconstructed mean annual temperature and pollen-reconstructed total annual precipitation from Suigetsu. Green horizontal bars indicate approximate boundaries between MIS 6, TII and MIS 5e, based on the pollen-reconstructed average annual temperature.

relating to the estimation of alpha efficiency, grain size and internal grain activity) and ED_e calculation (given that the samples are not mineralogically pure and only two aliquots were measured per fraction). However, these estimations do suggest that the PMF-IR signal is better suited as an environmental tracer, and that the QF-blue and PMF-blue signals show greater chronometric accuracy.

5. Discussion

5.1. Luminescence characteristics and environmental change

Throughout all four time periods it was possible to quantify a range of luminescence characteristics from the Suigetsu sediments. In most cases, the trends detected by the POSL and lab profiling approaches were very similar, and both techniques identified the same key environmental shifts in each of the four periods. The differences between the POSLnet and PIRSLnet profiles and the ED_e profiles can be attributed to variations in sensitivity, and as such, it could be argued that by removing the sensitivity component, the lab profiling approach provided a more accurate representation of down-core luminescence characteristics and should be the principal methodology for future studies. Moreover, the lab profiling analysis was conducted on chemically treated fractions with better (albeit not perfect) mineralogical constraint, which, by virtue, provides more accurate ED_e values. However, the POSL approach provided a more comprehensive suite of measurements (including depletion indices and PIRSL/POSL) which have the potential to capture a broader range of environmental shifts (albeit that they did not serve this function within the context of the present study). Additionally, the trends were clearer when a more intense, contiguous sampling approach (such as that used for Time Periods 1 and 3) was used, as this provided key contextual information and continuous data across transitions. The POSL approach is more suited to this type of sampling because it allows for rapid, non-destructive measurement of samples without a requirement for chemical preparation. Furthermore, the POSL analysis was conducted on larger samples (reducing geostatistical scatter). As a result, using both methods in a paired approach has advantages, as this offers both a more accurate determination of luminescence characteristics and a breadth of proxies for consideration. However, if large quantities of samples are necessary to clearly isolate trends, then the POSL approach is demonstrably sufficient for this purpose, especially in conjunction with complementary data. Calibrating the sensitivity of the POSL using an external radiation source could offer a means to ascertain sensitivity-corrected approximations of estimated equivalent dose whilst minimising processing time for large sample quantities (Munyikwa and Brown, 2014; Stone et al., 2015).

The principal signals seen in the key variables: POSLnet; PIRSLnet and ED_e were interpreted as relating to the different predominant environmental factors in each of the four time periods, allowing us to well-characterise the effects (and non-effects) of a range of distinctive perturbations. Hence, any common drivers between the time periods were masked by high amplitude variations of a single driver in each case. Differences in sampling approaches also preclude common interpretation of the variables as a result of different intervals between samples (and hence probing the variables on different timescales), amounts of integrated time within each sample (providing different weightings to single event layers) and the proficiency of contiguous versus spot-sampling approaches to identify trends on different scales, as discussed above. Not all of the luminescence variables could be attributed to a specific environmental change, however this could be due to our incomplete understanding of past catchment changes. Further "ground-truthing" of these proxies is required in other lacustrine settings (building on the work of Píšková et al. (2019)) to extend the applicability of this technique elsewhere. Nonetheless, it is highly promising that some of the selected variables were sensitive to known catchment changes, and that drivers could be hypothesised for other variables. This shows that by using POSL and lab profiling analysis, it was possible to gain further insight into environmental change at Suigetsu.

5.2. Assessment of dating potential

Future luminescence dating of the Suigetsu cores is feasible based on

the approximations of ED_e and ED_R shown above. All the samples from Time Periods 3 and 4 (which are older than the limit of radiocarbon dating, and hence targets for future dating) produced quantifiable natural signals. Responses were consistently measurable for large doses (50 Gy) but not small (5 Gy), suggesting that the grains are low in sensitivity, but not insufficiently sensitive so as to preclude future construction of dose response curves. A comparison of quartz and polymineral chronometric accuracy tentatively suggested that the QF-blue and PMF-blue signals were consistent with the existing Suigetsu chronology. Hence, blue light OSL dating of quartz is one possible future dating method (because the QF-blue fraction was highly dominated by quartz), however, the QF-blue fraction showed lower sensitivities and the quantity of quartz within the sediment was lower than other mineralogies. A key consideration for sampling will be how this (alongside the availability of core material) will direct sampling. Another possible method is blue light OSL dating of feldspar. The luminescence signal of felspars dominates the PMF-blue signals (which showed good chronometric accuracy) from Suigetsu because of the low abundance and sensitivity of quartz within the PMF-blue fraction (which therefore contributes very small amounts of signal). The PMF-IR signals consistently overestimated the age of the material and hence will not be suitable for dating (however, these signals are valuable contributors of information regarding catchment environmental change).

Additional considerations for dating are a better appraisal of quartz saturation via the construction of dose response curves, and an assessment of the feldspar fraction for evidence of incomplete bleaching to avoid an over-estimate of age. Further to this, it will be important to refine any calculations of dose rate; particularly by quantifying decay series disequilibrium (through alpha spectrometry) and developing a model of water content variability in order to reduce age uncertainty. Additionally, in light of the other key finding of this study (that luminescence signals from this material are influenced by environmental change), it would be incorrect to interpret any calculations of age as if this were not the case. Careful sampling (e.g., by avoiding the sampling of flood layers) will be vital when looking to determine full OSL ages for the Suigetsu cores, as will making use of further luminescence profiling to characterise these effects around target horizons for dating. Despite these complexities, the evidence suggests that luminescence dating can contribute accurate, meaningful age information to the current Suigetsu age-depth model.

6. Conclusions

A combined approach of POSL analysis and lab profiling provided a complementary suite of variables which detected a range of environmental changes at Lake Suigetsu, Japan. Across the four time periods, the luminescence characteristics of the sediment showed a clear response to flood events (Time Period 1) and the initiation of varving (Time Period 3), and broad fluctuations which coincided with variations in magnetic palaeointensity (Time Period 2) and a complex response to environmental changes during Termination II (Time Period 4). There was no response of the luminescence proxies to the connection of Suigetsu to the Sea of Japan (Time Period 1). Local environmental perturbations which caused a sedimentological change across decadal to centennial timescales showed the clearest trends in the luminescence profiles when probed with contiguous, high-resolution sampling. The value of these techniques in a lacustrine setting was demonstrated across a ~140,000-year age range. POSL analysis and lab profiling provide a practical solution to the time- and core material-constraints of traditional luminescence analysis, whilst allowing the detection of catchment-sensitive signals. The core material produced quantifiable luminescence signals and hence future luminescence dating is feasible. First order approximate ages from the PMF-IR signals suggest that these produce an overestimation of age, and hence future dating will target the QF-blue signal (which equates to blue light OSL dating of quartz) and PMF-blue signal (which equates to blue light OSL dating of feldspar), alongside a more accurate assessment of dose rate. The contribution of this work to our understanding of past dynamics at Lake Suigetsu demonstrates the applicability of rapid luminescence profiling of lake sediment cores for characterising past environmental change.

Research Data

Accompanying data from the POSL analysis, laboratory profiling analysis and dose rate estimates can be found at https://doi.org/10.5525/gla.researchdata.1263.

Declaration of competing interest

The authors declare that they have no known competing financial interests or personal relationships that could have appeared to influence the work reported in this paper.

Acknowledgements

This research did not receive any specific grant from funding agencies in the public, commercial, or not-for-profit sectors. CLR received funding from the NERC IAPETUS2 Doctoral Training Partnership. The SG06 core was recovered under NERC grant NE/D000289/1 awarded to TN. The authors would like to thank Dr Valerie Olive for performing the ICP-MS and ICP-OES analysis.

Appendix A. Supplementary information

Supplementary information relating to this article can be found online at https://doi.org/10.1016/j.quageo.2022.101319.

References

Albert, P.G., Smith, V.C., Suzuki, T., McLean, D., Tomlinson, E.L., Miyabuchi, Y., Kitaba, I., Mark, D.F., Moriwaki, H., , SG06 Project Members, Nakagawa, T., 2019. Geochemical characterisation of the Late Quaternary widespread Japanese tephrostratigraphic markers and correlations to the Lake Suigetsu sedimentary archive (SG06 core). Quat. Geochronol. 52, 103–131. https://doi.org/10.1016/j.quageo.2019.01.005.

Armitage, S.J., Pinder, R.C., 2017. Testing the applicability of optically stimulated luminescence dating to Ocean Drilling Program cores. Quat. Geochronol. 39, 124–130. https://doi.org/10.1016/j.quageo.2017.02.008.

Bateman, M.D., Catt, J.A., 1996. An absolute chronology for the raised beach and associated deposits at Sewerby, East Yorkshire, England. J. Quat. Sci. 11 (5), 389–395. https://doi.org/10.1002/(SICI)1099-1417(199609/10)11:5<389::AID-JQS260>3.0.CO;2-K.

Bronk Ramsey, C., Heaton, T.J., Schlolaut, G., Staff, R.A., Bryant, C.L., Brauer, A., Lamb, H.F., Marshall, M.H., Nakagawa, T., 2020. Reanalysis of the atmospheric radiocarbon calibration record from Lake Suigetsu, Japan. Radiocarbon 62 (4), 989–999. https://doi.org/10.1017/RDC.2020.18.

Bronk Ramsey, C., Staff, R.A.1., Bryant, C.L., Brock, F., Kitagawa, H., Van Der Plicht, J., Schlolaut, G., Marshall, M.H., Brauer, A., Lamb, H.F., Payne, R.L., Tarasov, P.E., Haraguchi, T., Gotanda, K., Yonenobu, H., Yokoyama, Y., Tada, R., Nakagawa, T., 2012. A complete terrestrial radiocarbon record for 11.2 to 52.8 kyr B.P. Science 338 (6105), 370–374. https://doi.org/10.1126/science.1226660.

Burbidge, C.I., Sanderson, D.C.W., Housley, R.A., Allsworth Jones, P., 2007. Survey of Palaeolithic sites by luminescence profiling, a case study from Eastern Europe. Quat. Geochronol. 2 (1–4), 296–302. https://doi.org/10.1016/j.quageo.2006.05.024.

Duan, W., Cheng, H., Tan, M., Li, X., Lawrence Edwards, R., 2019. Timing and structure of Termination II in north China constrained by a precisely dated stalagmite record. Earth Planet Sci. Lett. 512, 1–7. https://doi.org/10.1016/j.epsl.2019.01.043.

Gao, L., Gao, L., Yin, Y., Yu, G., Liao, M., 2017. Optical dating of Holocene tidal deposits from the southwestern coast of the South Yellow Sea using different grain-size quartz fractions. J. Asian Earth Sci. 135, 155–165. https://doi.org/10.1016/j.jseaes.2016.12.036.

Ghilardi, M., Sanderson, D., Kinnaird, T., Bicket, A., Balossino, S., Parisot, J.C., Hermitte, D., Guibal, F., Fleury, J.T., 2015. Dating the bridge at Avignon (south France) and reconstructing the Rhone River fluvial palaeo-landscape in Provence from medieval to modern times. J. Archaeol. Sci.: Report 4, 336–354. https://doi.org/10.1016/j.jasrep.2015.10.002.

Hu, G., Yi, C., Zhang, J., Cao, G., Pan, B., Liu, J., Jiang, T., Yi, S., Li, D., Huang, J., 2018. Chronology of a lacustrine core from Lake Linggo Co using a combination of OSL, 14C and 210Pb dating: implications for the dating of lacustrine sediments from the Tibetan Plateau. Boreas 47 (2), 656–670. https://doi.org/10.1111/bor.12291.

Hyodo, M., Nakagawa, T., Matsushita, H., Kitaba, I., Yamada, K., Tanabe, S., Bradák, B., Miki, M., McLean, D., Staff, R.A., Smith, V.C., Albert, P.G., Bronk Ramsey, C.,

Yamasaki, A., Kitagawa, J., Suigetsu 2014 Project Members, 2022. Intermittent non-axial dipolar-field dominance of twin Laschamp excursions. Commun. Earth Environ. https://doi.org/10.1038/s43247-022-00401-0.

Kadereit, A., DeWitt, R., Johnson, T.C., 2012. Luminescence properties and optically (post-IR blue-light) stimulated luminescence dating of limnic sediments from northern Lake Malawi - chances and limitations. Quat. Geochronol. 10, 160–166. https://doi.org/10.1016/j.quageo.2012.02.021.

Kinnaird, T.C., Sanderson, D.C.W., Bigelow, G.F., 2015. Feldspar SARA IRSL dating of very low dose rate aeolian sediments from Sandwick South, Unst, Shetland. Quat. Geochronol. 30, 168–174. https://doi.org/10.1016/j.quageo.2015.02.019.

Li, J., Yang, S., Shu, J., Li, R., Chen, X., Meng, Y., Ye, S., He, L., 2020. Vegetation history and environment changes since MIS 5 recorded by pollen assemblages in sediments from the western Bohai Sea, Northern China. J. Asian Earth Sci. 187 (October 2019), 104085. https://doi.org/10.1016/j.jseaes.2019.104085.

Long, H., 2012. High-resolution OSL chronology of a sediment core from Lake Nam Co on the southern Tibetan Plateau: implication for lake evolution since the late Glacial. Quat. Int. 279–280, 287–288. https://doi.org/10.1016/j.quaint.2012.08.762, 2012.

Marshall, M.H., Schlolaut, G., Nakagawa, T., Lamb, H.F., Brauer, A., Staff, R.A., Bronk Ramsey, C., Tarasov, P.E., Gotanda, K., Haraguchi, T., Yokoyama, Y., Yonenobu, H., Tada, R., 2012. A novel approach to varve counting using μXRF and X-radiography in combination with thin-section microscopy, applied to the Late Glacial chronology from Lake Suigetsu, Japan. Quat. Geochronol. 13, 70–80. https://doi.org/10.1016/j.quageo.2012.06.002.

McLean, D., Albert, P.G., Nakagawa, T., Suzuki, T., Staff, R.A., Yamada, K., Kitaba, I., Haraguchi, T., Kitagawa, J., Smith, V.C., 2018. Integrating the Holocene tephrostratigraphy for East Asia using a high-resolution cryptotephra study from Lake Suigetsu (SG14 core), central Japan. Quat. Sci. Rev. 183, 36–58. https://doi.org/10.1016/j.quascirev.2017.12.013.

Munyikwa, K., Brown, S., 2014. Rapid equivalent dose estimation for eolian dune sands using a portable OSL reader and polymineralic standardised luminescence growth curves: expedited sample screening for OSL dating. Quat. Geochronol. 22, 116–125. https://doi.org/10.1016/j.quageo.2014.04.002.

Munyikwa, K., Kinnaird, T.C., Sanderson, D.C., 2021. The potential of portable luminescence readers in geomorphological investigations: a review. Earth Surf. Process. Landforms 46 (1), 131–150. https://doi.org/10.1002/esp.4975.

Nakagawa, T., Gotanda, K., Haraguchi, T., Danhara, T., Yonenobu, H., Brauer, A., Yokoyama, Y., Tada, R., Takemura, K., Staff, R.A., Payne, R.L., Bronk Ramsey, C., Bryant, C.L., Brock, F., Schlolaut, G., Marshall, M.H., Tarasov, P.E., Lamb, H.F., 2012. SG06, a fully continuous and varved sediment core from Lake Suigetsu, Japan: stratigraphy and potential for improving the radiocarbon calibration model and understanding of late Quaternary climate changes. Quat. Sci. Rev. 36, 164–176. https://doi.org/10.1016/j.quascirev.2010.12.013.

Nelson, M., Rittenour, T., Cornachione, H., 2019. Sampling methods for luminescence dating of subsurface deposits from cores. Methods Protoc. 2 (4), 88. https://doi.org/10.3390/mps2040088.

Olive, V., Ellam, R.M., Wilson, L., 2001. A protocol for the determination of the rare earth elements at picomole level in rocks by ICP-MS: results on geological reference materials USGS PCC-1 and DTS-1. Geostand. Newsl. 25 (2-3), 219–228. https://doi.org/10.1111/j.1751-908X.2001.tb00597.x.

Pears, B., Brown, A.G., Toms, P.S., Wood, J., Sanderson, D., Jones, R., 2020. A sub-centennial-scale optically stimulated luminescence chronostratigraphy and late Holocene flood history from a temperate river confluence. Geology 48 (8), 819–825. https://doi.org/10.1130/G47079.1.

Píšková, A., Roman, M., Bulínová, M., Pokorný, M., Sanderson, D., Cresswell, A., Lirio, J. M., Coria, S.H., Nedbalová, L., Lami, A., Musazzi, S., 2019. Late-Holocene palaeoenvironmental changes at Lake Esmeralda (Vega Island, Antarctic Peninsula) based on a multi-proxy analysis of laminated lake sediment. Holocene 29 (7), 1155–1175. https://doi.org/10.1177/0959683619838033.

Porat, N., López, G.I., Lensky, N., Elinson, R., Avni, Y., Elgart-Sharon, Y., Faershtein, G., Gadot, Y., 2019. Using portable OSL reader to obtain a time scale for soil accumulation and erosion in archaeological terraces, the Judean Highlands, Israel. Quat. Geochronol. 49 (April 2018), 65–70. https://doi.org/10.1016/j.quageo.2018.04.001.

Rasmussen, S.O., Bigler, M., Blockley, S.P., Blunier, T., Buchardt, S.L., Clausen, H.B., Cvijanovic, I., Dahl-Jensen, D., Johnsen, S.J., Fischer, H., Gkinis, V., Guillevic, M., Hoek, W.Z., Lowe, J., Pedro, J.B., Popp, T., Seierstad, I.K., Steffensen, J.-P., Svensson, A.M., Winstrup, M., 2014. A stratigraphic framework for abrupt climatic changes during the Last Glacial period based on three synchronized Greenland ice-core records: refining and extending the INTIMATE event stratigraphy. Quat. Sci. Rev. 106, 14–28. https://doi.org/10.1016/j.quascirev.2014.09.007.

Saito-Kato, M., Yamada, K., Staff, R.A., Nakagawa, T., Yonenobu, H., Haraguchi, T., Takemura, K., Bronk Ramsey, C., 2013. An assessment of the magnitude of the AD 1586 Tensho tsunami inferred from Lake Suigetsu sediment cores. J. Geogr. 122, 493–501. https://doi.org/10.5026/jgeography.122.493 (in Japanese, with English abstract).

Sanderson, D.C., Kinnaird, T.C., 2019. Optically stimulated luminescence dating as a geochronological tool for late quaternary sediments in the red sea region. In: Rasul, N.M.A., Stewart, I.C.F. (Eds.), Geological Setting, Palaeoenvironment and Archaeology of the Red Sea. Springer, Cham, pp. 685–707. https://doi.org/10.1007/978-3-319-99408-6_31.

Sanderson, D.C.W., Murphy, S., 2010. Using simple portable OSL measurements and laboratory characterisation to help understand complex and heterogeneous sediment sequences for luminescence dating. Quat. Geochronol. 5 (2–3), 299–305. https://doi.org/10.1016/j.quageo.2009.02.001.

Schlolaut, G., Staff, R.A., Brauer, A., Lamb, H.F., Marshall, M.H., Bronk Ramsey, C., Nakagawa, T., 2018. An extended and revised Lake Suigetsu varve chronology from ~50 to ~10 ka BP based on detailed sediment micro-facies analyses. Quat. Sci. Rev. 200, 351–366. https://doi.org/10.1016/j.quascirev.2018.09.021.

Staff, R.A., Ramsey, C.B., Bryant, C.L., Brock, F., Payne, R.L., Schlolaut, G., Marshall, M. H., Brauer, A., Lamb, H.F., Tarasov, P.E., Yokoyama, Y., Haraguchi, T., Gotanda, K., Yonenobu, H., Nakagawa, T., 2011. New 14C determinations from Lake Suigetsu, Japan: 12,000 to 0 cal BP. Radiocarbon 53 (3), 511–528. https://doi.org/10.1017/S0033822200034627.

Stone, A.E.C., Bateman, M.D., Thomas, D.S.G., 2015. Rapid age assessment in the Namib Sand Sea using a portable luminescence reader. Quat. Geochronol. 30, 134–140. https://doi.org/10.1016/j.quageo.2015.02.002.

Zhao, G., Ye, S., Laws, E.A., He, L., Yuan, H., Ding, X., Wang, J., 2019. Carbon burial records during the last ~40,000 years in sediments of the Liaohe Delta wetland, China. Estuarine. Coast. Shelf Sci. 226 (July 2018), 106291. https://doi.org/10.1016/j.ecss.2019.106291.